Recombination-enhanced migration of interstitial aluminum in silicon

J. R. Troxell, A. P. Chatterjee, and G. D. Watkins
Department of Physics and Sherman Fairchild Laboratory, Lehigh University, Bethlehem, Pennsylvania 18015

L. C. Kimerling
Bell Laboratories, Murray Hill, New Jersey 07974
(Received 29 December 1978)

We report the first observation of recombination-enhanced recovery of a defect in silicon which is otherwise normally stable at room temperature. This defect, produced by 1.5-MeV electron irradiation of aluminum-doped material at room temperature, is identified as isolated interstitial aluminum through correlated deep-level transient-capacitance spectroscopy and EPR studies. The recovery rate constant in the absence of minority-carrier injection is $3(10^9)\exp(-1.2\pm0.1\ \text{eV/kT})\ \text{sec}^{-1}$. Under saturated injection conditions, it is $70\exp(-0.27\pm0.03\ \text{eV/kT})\ \text{sec}^{-1}$. This represents an enhancement of the recovery rate by a factor of $\sim 10^8$ at room temperature. We conclude that this enhancement results from an efficient conversion of the electronic energy available upon carrier capture to local vibrational energy of the defect which assists it over the migration barrier. The second donor level of the defect (Al_i^+/Al_i^{++}) is determined to be at $E_V + 0.17$ eV. We conclude, however, that the enhancement results from carrier capture and recombination at the first donor level (Al_i^0/Al_i^+) the position of which has not yet been determined. The implications of these results to the properties of the self-interstitial in silicon are discussed.

I. INTRODUCTION

Recently the phenomenon of recombination-enhanced defect migration has become recognized as an important factor for defects in many semiconductors.[1-4] In GaP and GaAs, for instance, many of the defects produced by radiation damage have been found to exhibit enhanced recovery under minority-carrier injection conditions.[5-9] This phenomenon is believed to play an important role in the degradation observed under injection conditions for many devices made from these materials. Similar effects have also been reported for ZnSe.[10]

Broadly speaking, the mechanism for this enhanced migration is that the electronic energy released upon carrier capture and recombination supplies part of the energy necessary for the defect to make a diffusional jump. In the III-V and II-VI materials, a band gap of several electron volts is available for this process. In silicon, on the other hand, the band gap is only 1.2 eV. Consistent with this, injection-enhanced motion in silicon has been reported[11-13] or conjectured[2,14] mainly only for defects stable at cryogenic temperatures (vacancies, interstitials, etc.) and not for defects stable at or above room temperature.[1,15,16]

In this paper, we report the first observation[17] of a room-temperature-stable defect in silicon which can be made to migrate under injection conditions. The process is remarkably energy efficient, approximately 0.9 eV being extracted to assist the motion, with the migration rate enhanced by a factor of $\sim 10^8$ under injection conditions at room temperature. The defect is identified as interstitial aluminum,[18] an important defect produced by radiation damage in aluminum-doped material.

In this study, we combine deep-level transient-capacitance spectroscopy (DLTS) with electron-paramagnetic resonance (EPR). EPR studies of interstitial aluminum in silicon were first reported in Ref. 19. There, the *G*18 spectrum was identified as belonging to the double-donor charge state of interstitial aluminum. The spectrum was found to exhibit T_d symmetry, indicating that the aluminum atom sits on the normal tetrahedral interstitial site within the silicon lattice. This spectrum was found to be stable to above 200 °C, when it was replaced with new spectra (*G*19, *G*20, *G*21) which were found to involve aluminum atoms complexed with other defects. In particular the identification of the *G*19 and *G*20 spectra as belonging to aluminum-interstitial–aluminum-substitutional pairs indicated that the recovery process involved long-range migration of the interstitial aluminum. In the present study, we confirm directly by EPR that the same long-range migration process occurs under the injection-enhanced conditions. By detailed correlation with DLTS, a quantitative study of the effect is made.

The role of recombination-enhanced migration in silicon has been a subject of considerable interest as a possible explanation of the remarkable apparent mobility of interstital silicon during electron irradiation at cryogenic temperatures.[2,14,20] In *p*-type silicon irradiated by high-energy electrons at 4.2 K, no isolated interstitial silicon

atoms have been detected. Instead only dopant interstitials (boron, aluminum) are observed, in approximate one-to-one correspondence to isolated vacancies.[19] This has led to the suggestion that long-range ionization-enhanced motion of the silicon interstitials has occurred, with trapping by the substitutional impurities to produce interstitial impurities by replacement.

The insight gained by our study here of interstitial aluminum allows us to speculate on the mechanism of interstitial silicon migration.

II. EXPERIMENTAL PROCEDURE

Samples were fabricated from floating-zone-grown silicon doped with 1.5×10^{16} aluminum/cm^3. Both bulk EPR samples (approximately $0.25 \times 0.25 \times 1.25$ cm) and {110} wafers (0.025 cm thick) were sliced from the same boule. Asymmetric abrupt junctions were fabricated for DLTS studies on the polished wafers in three ways: (i) Schottky barriers were produced by high-vacuum deposition of silver through a metal mask. (ii) Diffused n^+p junctions were prepared by standard high-temperature oxidation and phosphorus diffusion procedures. Due to the high diffusivity of oxygen in silicon, these devices presumably contained a significant amount of oxygen in the depletion region. (iii) Ion-implanted n^+p junctions were fabricated, in order to avoid the introduction of oxygen into the junction region. These involved low-temperature (450 °C) chemical vapor deposition of SiO_2 for masking, phosphorus-ion implantation (90 keV), and subsequent annealing in an inert atmosphere at 850 °C. Devices were then diced apart and mounted on TO-5 headers. Electrical connections were made by ultrasonic bonding. Prior to electron irradiation, no deep-level DLTS spectra[21,22] were seen.

The samples were mounted on a water-cooled block and irradiated with an external beam of 1.5-MeV electrons from a General Electric resonant transformer accelerator. The flux was low enough to keep sample temperatures near room temperature during the irradiation. The DLTS samples were irradiated to a fluence[23] of 5×10^{15} e/cm^2. The EPR samples were irradiated to larger fluences,[23] 1.5×10^{16} and 5×10^{16} cm^{-2} in order to increase the intensity of the EPR signals.

The electrical properties of the diode samples were then studied by DLTS with an apparatus similar to that described by Lang.[21,22] Minority-carrier injection was obtained by either forward biasing the n^+p diode structures or by illuminating the Schottky diodes with 1.064-μm light from a Nd-YAG (Sylvania Model 607) laser through windows etched in the back metallization. The narrow width of the junction depletion region (~1 μm) ensured that in both cases the density of minority carriers was approximately uniform.

In the case of the thicker EPR samples, 1.064-μm laser light was used to supply minority-carrier injection. During illumination, the samples were cooled by chilled compressed air. The absorption coefficient of the samples at 1.064 μm was measured directly during the illumination to be 13.7 cm^{-1}. Using published values of the absorption coefficient versus temperature at this wavelength,[24] the temperature during the laser illumination was estimated to be 320 K. With this absorption coefficient, the light intensity has dropped to 20% in the center of the crystal and to 4% at the far side. The crystals were therefore illuminated equally from two opposite sides providing a symmetric intensity profile that has dropped to 40% intensity in the middle. Uniform illumination of each surface was supplied by sweeping the laser beam (3.75 W, ~3-mm-diam spot) uniformly along the length of the samples.

For most of the studies, the EPR signals were monitored at 20.4 K in dispersion with 94 Hz (f_m) magnetic field modulation, lock-in detection, and recording. The lines were inhomogeneously broadened, with adiabatic fast passage through the spin packets giving absorptionlike spectra.[25,26] At this temperature the passage cases for the different signals differed, some with $\omega_m T_1 > 1$, others with $\omega_m T_1 < 1$. Monitoring at this temperature therefore sufficed for studying the relative changes in intensity of the spectrum for each individual defect separately versus radiation flux, recovery, etc., but could not supply reliable relative concentrations for spectra from different defects. To establish this calibration, the temperature was varied by pumping on the liquid hydrogen (10–20.4 K) to bring each spectrum into the same passage case, $\omega_m T_1 \gg 1$. Area measurements under each of the recorded spectra under the identical passage case[25,26] and spectrometer conditions (H_1, ω_m, H_m) were then taken and corrected by the Boltzmann factor (different temperatures) to give the relative concentrations of the corresponding defects. This calibration, done once, supplied multiplicative correction factors for the amplitudes determined routinely at 20.4 K to convert them to relative concentration between the defects.

Annealing of the diodes above 100 °C was performed in a temperature-regulated oil bath. Below 100 °C the samples were annealed *in situ* in the DLTS apparatus, the temperature being regulated by balance between the flow of cooling gas from liquid nitrogen and a heater around the sample holder.

III. EXPERIMENTAL RESULTS

A. DLTS Studies

As seen in Fig. 1, the irradiated samples exhibit four dominant majority-carrier (hole) traps, three of which ($H2$, $H3$, $H4$) have been observed only in aluminum-doped material. The $H1$, $H2$, and $H3$ levels are observed to be produced in approximately the same relative concentrations in Schottky, ion implanted and diffused junctions. The $H4$ level, on the other hand, is found to be reduced in concentration in the diffused junctions. The $H4$ level has been tentatively identified by Kimerling[16] as associated with the aluminum-vacancy pair. This identification is consistent with our results, the reduced intensity in the diffused junctions being consistent with a competition for vacancy trapping with oxygen unavoidably introduced in the diffused junction processing. The previous identification of the $H1$ level as a state of the divacancy[16] will be shown to be reinforced by our results. The identity of $H2$ is at present unknown. Studies to unravel the nature of this level are currently in progress.[27]

In this paper we will be concerned with the defect level $H3$ which, in agreement with the tentative identification by Kimerling,[16] we identify as corresponding to the double donor level of interstitial aluminum. As shown in Fig. 1, this level can be annealed at room temperature under minority-carrier injection, even though it is otherwise stable to above 200 °C. Therefore, although the $H3$ spectrum strongly overlaps that of $H2$, it can be fully resolved by subtracting injection from unannealed spectra. This technique was employed in the following characterization of the $H3$ level.

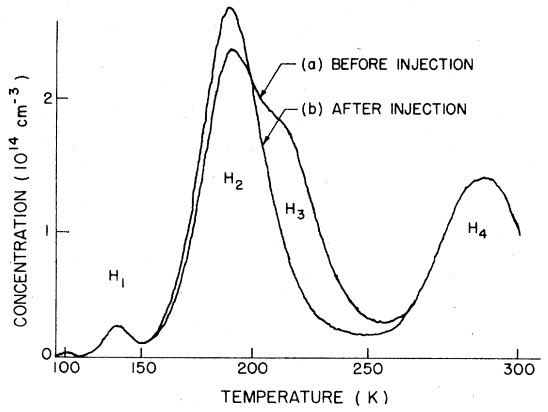

FIG. 1. DLTS spectrum [$\tau = 9 \times 10^{-4}$ sec] of phosphorus ion-implanted junction on aluminum-doped (1.5×10^{16} cm^{-3}) silicon substrate following room-temperature irradiation and 100 °C thermal anneal. (a) Following irradiation we find four dominant defect levels. (b) After forward bias injection (3.6 A/cm^2, ~30 min, 300 K) defect level $H3$ has recovered.

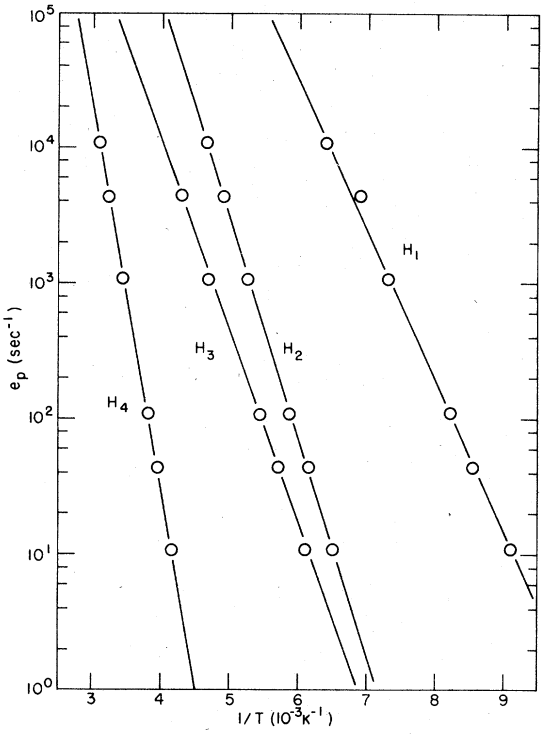

FIG. 2. Temperature dependence of the hole emission rates for the defects in Fig. 1.

The temperature dependence of the hole emission rates of the four levels is shown in Fig. 2. For the levels, we find

$$\begin{aligned} e_p(H1) &= 1 \times 10^{11} \exp(-0.22 \pm 0.01 \text{ eV}/kT) \text{ sec}^{-1}, \\ e_p(H2) &= 3 \times 10^{11} \exp(-0.32 \pm 0.01 \text{ eV}/kT) \text{ sec}^{-1}, \\ e_p(H3) &= 5 \times 10^{9} \exp(-0.28 \pm 0.01 \text{ eV}/kT) \text{ sec}^{-1}, \\ e_p(H4) &= 6 \times 10^{12} \exp(-0.56 \pm 0.01 \text{ eV}/kT) \text{ sec}^{-1}. \end{aligned} \tag{1}$$

Thus we obtain a first-order estimate of the $H3$ defect energy level as 0.28 ± 0.01 eV above the valence band. To refine this estimate we must account for the influence of other temperature-dependent terms which relate a trap's energy level and its carrier emission rate.

This relation is obtained through an application of the principle of detailed balance to the carrier interactions with the defect level, which results in the familiar equation

$$e_p = (v_{\text{th}} N_V \sigma_p g) \exp[-(E_T - E_V)/kT], \tag{2}$$

where N_V represents the effective-mass density of states in the valence band, σ_p the hole-capture cross section, v_{th} the thermal velocity of the carriers [$= (3\ kT/m^*)^{1/2}$] and $(E_T - E_V)$

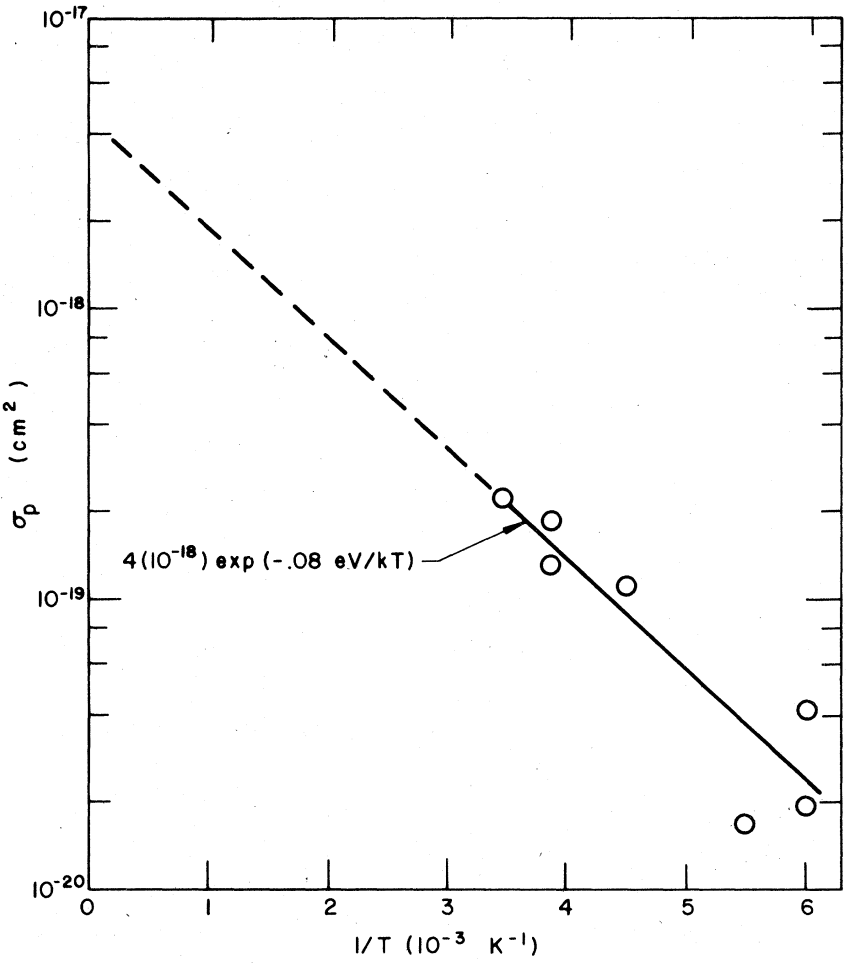

FIG. 3. Temperature dependence of the hole capture cross section for the $H3$ defect level.

the defect level position above the valence-band edge. The defect energy-level degeneracy (g) represents a relatively small correction to the emission rate and will be neglected in the following.

Together, the effective-mass density of states and the thermal velocity exhibit a quadratic dependence upon temperature, effectively contributing 0.03 eV to the measured hole emission activation energy. The temperature dependence of the hole-capture cross section has been measured for the $H3$ defect level using a technique described by Lang.[21] This involves directly measuring the hole capture rate c_p at the trap by varying the width of the trap-filling pulse, and obtaining the hole-capture cross section from

$$c_p = \sigma_p v_{\text{th}} p\,, \tag{3}$$

where p is the concentration of holes. For the $H3$ defect (Fig. 3) we find a small hole-capture cross section which exhibits a temperature dependence

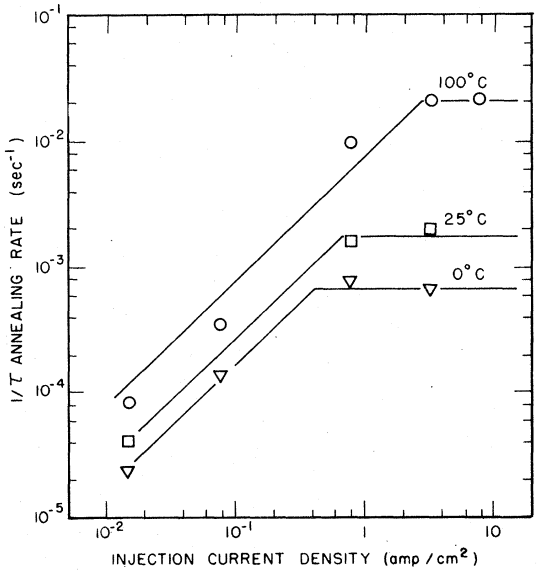

FIG. 4. $H3$ defect recovery rate as a function of injection current density at 0, 25, and 100 °C.

with an activation energy of 0.08 ± 0.03 eV. As a result, we estimate the true energy-level position[28] of the $H3$ trap:

$$E_T - E_V = 0.28 \pm 0.01 - 0.03 - 0.08 \pm 0.03$$
$$= 0.17 \pm 0.04 \text{ eV}. \quad (4)$$

A study of the recovery rate of the $H3$ defect level as a function of injection current density leads to the results shown in Fig. 4. For low injection currents, the $H3$ recovery rate is linearly proportional to the injected current density. At higher current densities (greater than ~1 A/cm^2) the recovery rate saturates.

The recovery kinetics of the $H3$ defect have been studied under saturated injection conditions, and the results are given in Fig. 5. Also shown are the results for the defect with no injection (shorted junction). In each of these studies, the recovery followed a simple exponential decay with time constant τ, given by

$$\tau^{-1}_{\text{sat inj}} = 70 \exp(-0.27 \pm 0.03 \text{ eV}/kT) \text{ sec}^{-1}, \quad (5a)$$

$$\tau^{-1}_{\text{no inj}} = 3 \times 10^9 \exp(-1.2 \pm 0.1 \text{ eV}/kT) \text{ sec}^{-1}. \quad (5b)$$

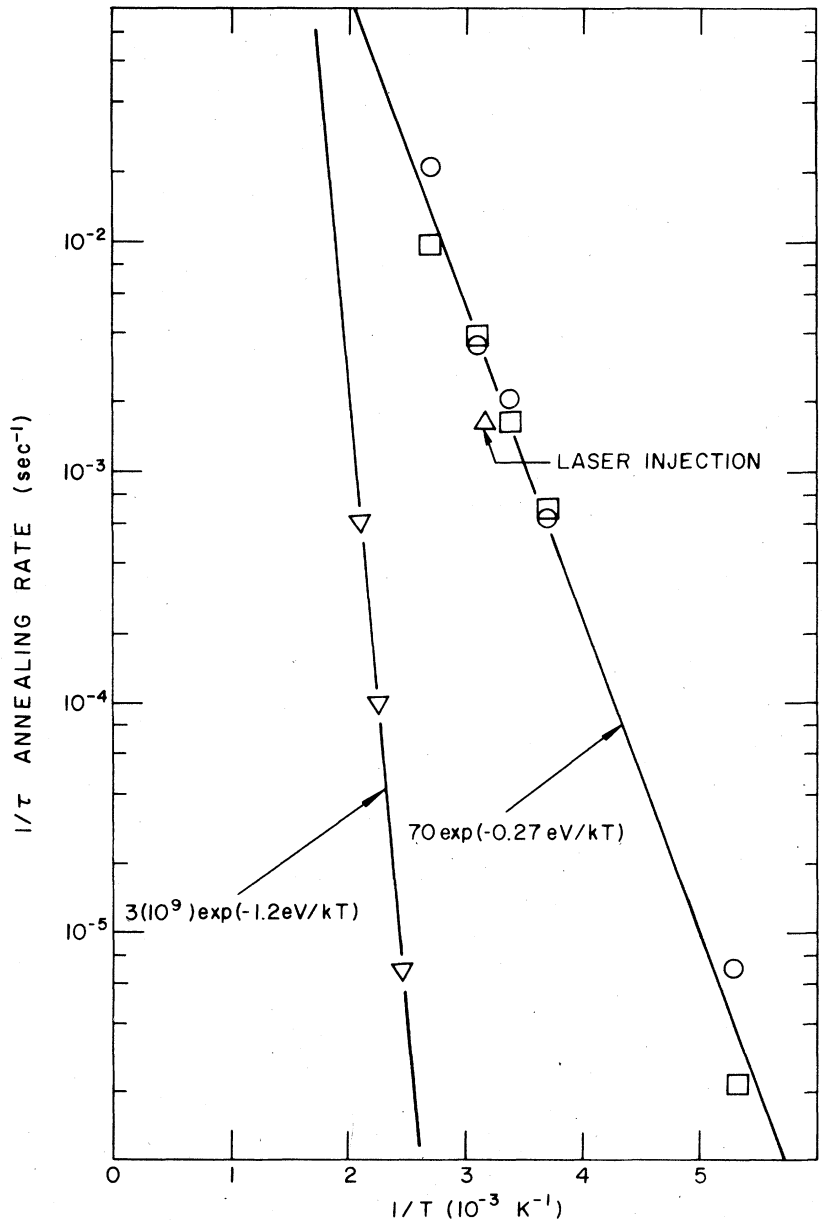

FIG. 5. Temperature dependence of the recovery rate of the $H3$ defect, (a) under short-circuit conditions (▽), (b) under saturated forward bias injection conditions (□, 0.8 A/cm^2; ○, 3.6 A/cm^2). Also shown (△) is the result for recovery at 320 K under Nd-YAG laser illumination.

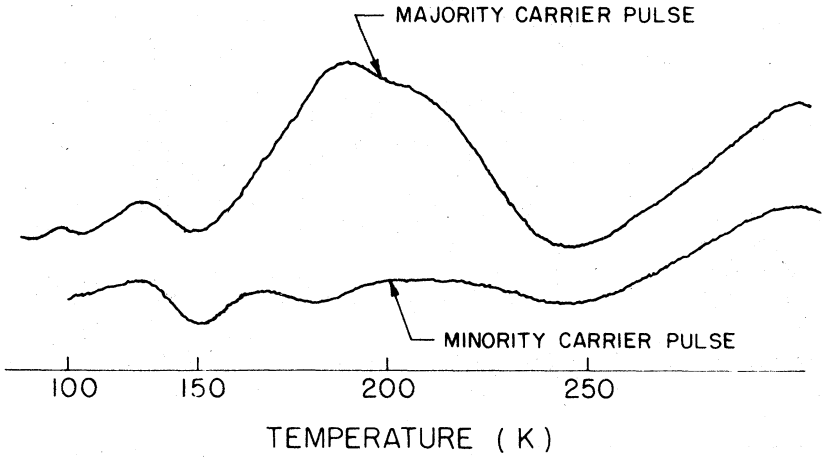

FIG. 6. Standard DLTS spectrum (trap filling pulse introduces only majority carriers) and minority-carrier spectrum (trap filling pulse forward biases junction). It is found that an injection current density of only $\sim 10^{-3}$ A/cm^2 is sufficient to erase the $H3$ (and $H2$) defect peaks from the spectrum.

Thus, the introduction of minority carriers is apparently responsible for supplying ~0.9 eV of energy towards the 1.2 eV normally needed for defect migration. (That long-range defect migration is in fact the mode of recovery which will be shown later.) At injection levels below saturation, the experimental results are less accurate. We may estimate the recovery kinetics in this region (for $J=0.1$ A/cm^2),

$$\tau^{-1}_{0.1\ \mathrm{inj}} \simeq 6\times 10^{-2}\exp(-0.14\ \mathrm{eV}/kT)\ \mathrm{sec}^{-1}. \quad (5c)$$

In Fig. 6, we show the DLTS spectrum under injection conditions during the pulse. No well-resolved minority-carrier traps are observed. On the other hand, injection current densities as low as ~10^{-3} A/cm^2 are sufficient to erase the $H2$ and $H3$ peaks. This means that the levels are being saturated with minority carriers, implying large electron-capture cross sections.

In order to correlate the electrical measurements studies with those using EPR, to be described in Sec. III B, we also examined recovery of DLTS samples under the same laser illumination conditions which were applied to the bulk EPR samples. Under these conditions (Fig. 5) we observed a recovery rate close to the saturated recovery rate found by forward bias injection.

B. EPR Studies

Immediately after electron irradiation the dominant EPR spectra observed are divacancies ($G6$),[29] carbon interstitials ($G12$),[30] aluminum interstitials ($G18$),[19,31] and aluminum-vacancy pairs ($G9$).[32] The aluminum-vacancy pairs are observed in a photoexcited $S=1$ state and it is therefore not possible to determine the relative concentration of these defects from the intensity of the spectrum. On the other hand, the remaining defects give $S=\frac{1}{2}$ spectra, are paramagnetic in the ground states of their normal charge states in the p-type material, and their relative concentration could therefore be determined as indicated in Fig. 7.

The results of laser illumination at 320 K are also given in the figure. The rapid conversion of the carbon interstitials ($G12$) to carbon-inter-

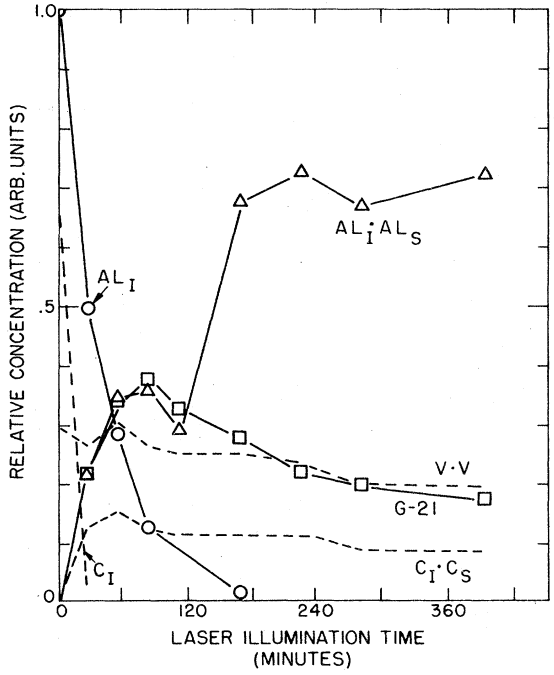

FIG. 7. Relative defect concentrations (determined from EPR) vs Nd-YAG laser illumination time (on each side) at 320 K. The $C_i \rightarrow C_iC_s$ conversion results from normal thermal recovery at this temperature and is not an ionization enhanced effect.

stitial–carbon-substitutional pairs ($G11$) can be accounted for purely by the known thermal recovery kinetics[30] for this process at 320 K and serves to confirm the estimate of the sample temperature during laser illumination. It is not therefore an ionization-enhanced effect. (Interstitial carbon has also been observed in the DLTS studies as a poorly resolved shoulder on the low-temperature side of $H2$—corresponding to a peak at 170 K in Fig. 1. The DLTS sample in Fig. 1 had been recovered at 100°C for 30 min in order to remove it.) On the other hand, the disappearance of interstitial aluminum with the corresponding growth of one of the aluminum-interstitial–aluminum-substitutional pairs ($G19$) and the $G21$ spectrum[33] must be attributable to the ionization. The corresponding thermal recovery does not occur until ~200°C.[19] At the same time, the concentrations of divacancies, carbon-carbon pairs, and aluminum-vacancy pairs do not change appreciably.

The conversion of interstitial aluminum to the aluminum pairs and the $G21$ spectrum in Fig. 7 is similar to that observed in thermal anneals at ~200°C. The defect giving rise to the $G21$ spectrum has not been identified but it is known to involve aluminum as revealed by its $I=\frac{5}{2}$ hyperfine structure. On the other hand, the identification of the $G19$ spectrum as aluminum-interstitial–aluminum-substitutional pairs clearly demonstrates that the recovery involves long-range interstitial-aluminum migration as had been previously concluded from the high-temperature recovery studies.[19]

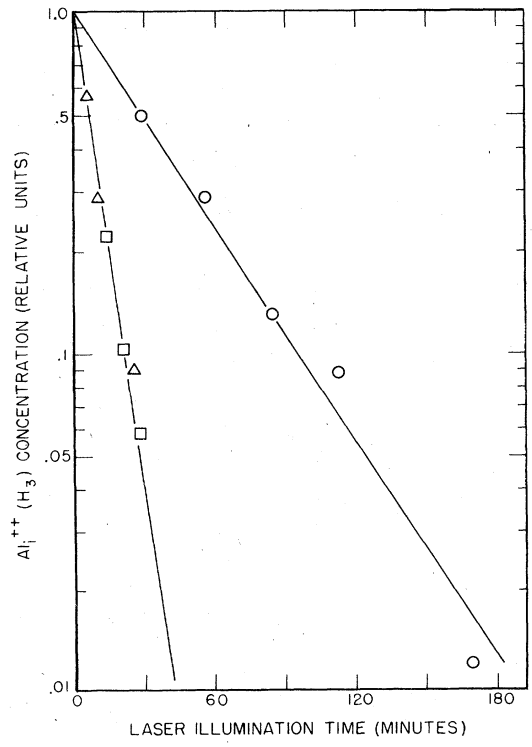

FIG. 8. Comparison of the laser-induced recovery kinetics of interstitial aluminum for EPR studies [□, ~1.5×10^{16} e/cm^2, ○, ~5×10^{16} e/cm^2] and DLTS studies (△, ~5×10^{15} e/cm^2) (see Ref. 23).

The EPR measurements of Fig. 7 were performed in samples which were electron irradiated to a fluence of 5×10^{16}/cm^2 in order to increase the amplitude of the EPR signals. Figure 8 shows also the results of the interstitial-aluminum recovery for a sample of 1.5×10^{16} e/cm^2 fluence, conditions closer to those for the DLTS samples (5×10^{15} e/cm^2).[23] As seen in the figure, the laser-induced recovery behavior for this sample is essentially identical to that of the DLTS samples. Thus we have a direct quantitative correlation between the $H3$ defect level observed in DLTS and the interstitial-aluminum spectrum observed by EPR.

In Fig. 7, we note that initially the relative concentration of interstitial aluminum to divacancies is about 3:1, which is what we observe in the DLTS spectra as the relative concentration of $H3$ to $H1$. This lends support to the previous identification of $H1$ as the donor level of the divacancy.[16]

IV. DISCUSSION

A. Identity of the $H3$ (0.17) DLTS level

The $H3$ level is observed only in irradiated aluminum-doped material. It is observed in the same relative concentration compared to the $H1$ level (identified as the divacancy[16]) as interstitial aluminum to divacancies determined directly from EPR studies. The thermally activated and injection-enhanced recovery of the level display a direct 1:1 correlation with the recovery of interstitial aluminum observed in the EPR studies. We conclude therefore that the defect responsible for the $H3$ level is interstitial aluminum. From EPR studies, it is known that the normal charge state in p-type material is Al_i^{++}. This identifies the $H3$ level at E_V +0.17 eV as the second donor state (Al_i^{+}/Al_i^{++}) of interstitial aluminum.

B. Injection-enhanced migration

1. Mechanisms

Mechanisms for injection-enhanced defect migration have recently been reviewed by

several authors.[1-4] Typically, three different mechanisms have been considered.

(i) *Charge-state mechanism.* Here the barrier for migration is lower in a second charge state of the defect which is generated under the injection conditions. Charge-state dependence of migration energies has been established for isolated vacancies,[34] phosphorus-vacancy pairs,[35] and antimony-vacancy pairs[36] in silicon.

(ii) *Saddle-point (Bourgoin[20]) mechanism.* Here the stable configuration for one charge state is the saddle point for migration of another charge state, and vice versa, the defect making one diffusional jump on the average for every two charge-state change cycles. (Half the time, the defect hops back.) No example of this mechanism has been established so far in semiconductors but the F_A(II) centers in alkali halides display much of these features.[37]

(iii) *Energy-release mechanism.* Here the electronic energy release available upon capture of a carrier is converted to vibrational energy of the defect which assists it over the barrier. This has also been labeled the *recombination-enhanced* mechanism[1] because recombination of electrons and holes is usually the principal process by which a defect repetitively captures carriers during injection conditions. An example of this has been established for one defect in GaAs[5,6] and strong evidence has been presented for several other defects in GaAs[7] and GaP.[8]

Mechanisms (i) and (ii) have in common the fact that they result from a charge-state change but do not depend upon the mechanism by which the change occurs. Mechanism (iii) on the other hand depends upon the electronic energy release and therefore may depend critically upon the nature of the electronic transition involved.

2. Al_i^+/Al_i^{++} *second donor state*

We can rule out immediately mechanisms (i) and (ii) at the $H3$ level because of its stability at room temperature. From Eq. (1), it is emitting holes at a rate of $\sim 10^5$ sec^{-1} at 300 K. The measured hole-capture rate at this temperature is also about 10^5 sec^{-1} which means that interstitial aluminum is changing its charge state from (+) to (++) and back again at $\sim 10^5$ sec^{-1}.[38] If mechanisms (i) or (ii) were operative, interstitial aluminum would therefore not be stable at room temperature.

Now consider mechanism (iii) at the $H3$ level. The dependence of the enhanced recovery rate on injected current density given in Fig. 4 implies that both electron capture and hole capture are involved in the process. For low injection currents, the linear dependence upon injected electron concentration indicates that the enhanced recovery process is limited by the electron-capture rate, $\sigma_n n v_{th}$. Above saturation, the process becomes limited by the hole-capture rate, $\sigma_p p v_{th}$, which is constant, reflecting the constant hole concentration of the p-type material. At the saturation point, ~ 1 A/cm^2, the electron- and hole-capture rates responsible for the enhanced migration are approximately equal. This does not correspond, however, to the injection level where electron- and hole-capture rates are equal for the $H3$ level, as indicated by the results of Fig. 6. There we found that the $H3$ DLTS signal could be erased, and therefore the electron- and hole-capture rates made equal at only ~ 1 mA/cm^2. We conclude therefore that the enhanced migration is *not* taking place as a result of capture of electrons or holes at the $E_V + 0.17$ eV second donor level responsible for the $H3$ DLTS spectrum.

3. Al_i^0/Al_i^+ *single donor level*

We are led to conclude that the enhanced migration must reflect the properties of another level associated with interstitial aluminum. It is of course reasonable to assume that a single donor (0/+) state also exists, since most point defects exhibit a neutral charge state within the energy gap. The fact that such a level is not seen as a hole trap in our DLTS studies implies that the single donor level must lie in the upper half of the gap. As such, this level would remain empty of electrons except under injection conditions. Let us consider again therefore each of the three mechanisms as related to the single donor level (0/+) of the interstitial aluminum. These mechanisms are illustrated by the simplified configuration coordinate diagrams of Fig. 9.

(i) *Charge-State Mechanism.* In this case, enhanced migration is occurring by thermal excitation over the barrier E_B' in the neutral state as illustrated in Fig. 9(a). (The defect thermalizes quickly at the equilibrium coordinate Q' and does not utilize any of the capture energy E_R' to assist it in its motion.) Saturation injection conditions imply complete conversion to the neutral state[39] and the observed activation energy for recovery (0.27 eV) would therefore be equal to E_B'. In this case, we would expect the preexponential factor for the recovery rate to be of the order of the lattice vibrational frequency ($\sim 10^{13}$ sec^{-1}) divided by the number of migrational jumps required until the defect be-

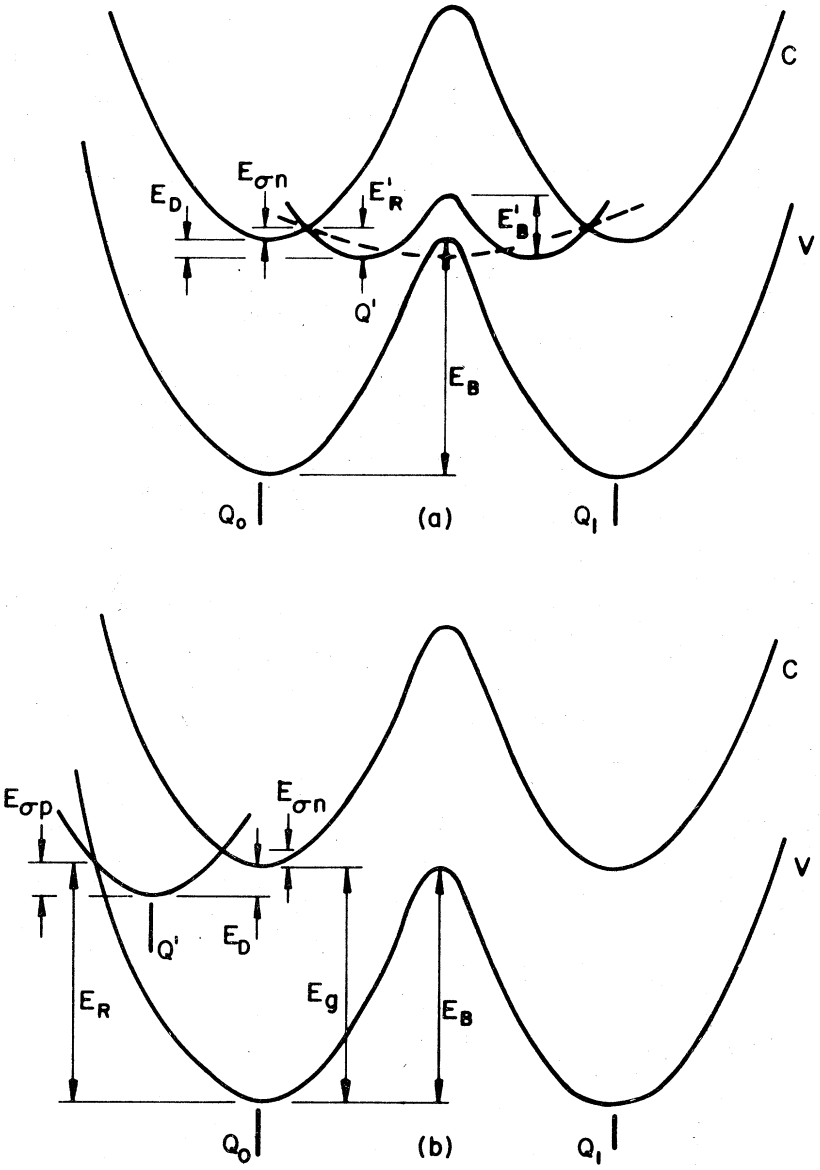

FIG. 9. Two possible configuration coordinate diagrams for the Al_i^0/Al_i^+ donor state. For each, the three energy contours represent the total energy (electronic plus elastic) for the defect with an electron either at the top of the valence band, the bottom of the conduction band, or trapped at the defect. The coordinate Q represents displacement of the atom from the normal tetrahedral site Q_0 along a line connecting it to an adjacent empty tetrahedral site Q_1. Shown dotted in (a) is the filled trap contour for a saddle-point migration mechanism.

comes trapped ($N_J \sim 10^6$) yielding $\tau_0^{-1} \sim 10^7$ sec^{-1}. The thermal recovery we observe without injection, Eq. (5b), is typical of this, having a preexponential factor of 3×10^9 sec^{-1}. Under injection conditions, however, the small observed preexponential factor, Eq. (5a), of 70 sec^{-1} appears incompatible with this explanation. We therefore rule out the charge-state mechanism at the single donor level.

(ii) *Saddle-point mechanism.* This is illustrated by the dashed neutral-state energy contour in Fig. 9(a), the minimum energy point being halfway between the two interstitial sites. The figure illustrates the interesting point that, in this case, the barrier for Al_i^+ thermally activated motion should not exceed $E_g - E_D$, because the ion could release a hole when the single donor state crosses the valence band, allowing it to make the diffusional transition along the lower-energy dotted path for the neutral state. The fact that the measured energy barrier[40] is 1.2 ± 0.1 eV in the absence of injection[41] requires therefore that E_D for the saddle point be 0 ± 0.1 eV.[42] It is therefore only the uncertainty in the measured barrier that allows a bound saddle-point state at all.

Saturation under injection conditions again means that complete conversion to the neutral

state has occurred and that the rate of charge-state change is being limited by the $Al_i^0 \rightarrow Al_i^+$ conversion processes. For a defect this shallow ($E_D < 0.1$ eV), the most likely process for this conversion is electron emission which would have a rate, in analogy to Eq. (2),

$$e_n = \sigma_n N_c v_{th} \exp(-E_D/kT) .$$

Including a temperature dependence of the electron-capture cross section in order to reflect the capture barrier $E_{\sigma n}$ yields

$$e_n = \sigma_{n0} N_c v_{th} \exp[-(E_D + E_{\sigma n})/kT] . \quad (6)$$

For an intermediate temperature (298 K), $v_{th} = 2\times10^7$ cm/sec and

$$N_c = 2.8\times10^{19}(\tfrac{1}{300}T)^{3/2} = 2.8\times10^{19} \text{ cm}^3 .$$

The high-temperature limit of the electron-capture cross section σ_{n0} may be estimated to be $\sim10^{-15}$ cm^2, being of the order of an atomic dimension squared (such a value is typically found experimentally).[43] We thus estimate the preexponential factor in Eq. (6) as $\sim10^{12}$ sec^{-1}. Assuming $N_J \sim 10^6$ jumps are required for long-range migration recovery, this predicts a characteristic preexponential factor for carrier emission limited recovery of $\sim10^6$ sec^{-1}. Again, this is inconsistent with the observed preexponential factor of 70 sec^{-1}. We thus conclude that a saddle-point mechanism is not responsible for the enhanced recovery.

(iii) *Energy release mechanism.* Two possibilities exist: (a) the motion could occur upon electron capture, Fig. 9(a), the atom receiving the energy E_R' which assists it over the thermal migration barrier E_B' for the neutral site; (b) the motion could occur upon hole capture, Fig. 9(b), with E_R assisting it over the barrier E_B for the positive charge state. In either case, the analysis of Weeks *et al.*[44] and Kimerling[1,15] can be applied, giving for the recovery rate

$$\tau^{-1} = (C\eta/N_J)\exp[-(E_B - E_R)/kT] , \quad (7)$$

where E_B (or E_B') is the thermal migration barrier, E_R (or E_R') is the vibrational energy supplied upon carrier capture [$< E_B$ (or E_B')], C (or C') is the rate of the carrier capture,[45] and η is an efficiency factor which takes account of both the probability that the energy is channeled into the appropriate diffusive mode and the number of vibrational cycles that the energy is available before it is lost to the lattice. Including a temperature dependence for C reflecting a barrier for the relevant carrier capture E_σ, the recovery rate becomes

$$\tau^{-1} = (C_0\eta/N_J)\exp[-(E_B - E_R + E_\sigma)/kT] . \quad (8a)$$

If $E_B < E_R$, the result becomes

$$\tau^{-1} = (C_0\eta/N_J)\exp(-E_\sigma/kT) . \quad (8b)$$

Consider first case (b) where the motion is initiated by hole capture. Under saturated injection conditions interstitial aluminum is primarily in the neutral state giving

$$C_0 = \sigma_{p0} p v_{th} . \quad (9)$$

For $T = 373$ K, with $p = 1.5\times10^{16}$ cm^{-3}, $v_{th} = 2.4\times10^7$ cm/sec, and $N_J \sim 10^6$, the observed preexponential factor from Eq. (5a), 70 sec^{-1}, gives $\sigma_{p0}\eta \sim 2\times10^{16}$ cm^2. Assuming, as before, $\sigma_{p0} \sim 10^{-15}$ cm^2, we obtain $\eta \sim 0.2$, a reasonable value.

Alternatively, if the electron-capture process is the operative one, Fig. 9(a), we compare to the experimental results under minority-carrier-limited conditions, Eq. (5c), where

$$C_0' = \sigma_{n0} n v_{th} . \quad (10)$$

Following Henry *et al.*[46] we can obtain an estimate of the injected electron concentration

$$n = (\gamma J/q)(t_n/kT\mu_n)^{1/2} , \quad (11)$$

where γ is an injection efficiency (assumed to be 0.5), q, the electronic charge, J, the injection current density, t_n, the minority-carrier lifetime (assumed $\sim 10^{-6}$ sec), and μ_n, the electron mobility (~ 860 cm^2 V^{-1} sec^{-1}). For $T = 373$ K and $J = 0.1$ A/cm^2, we obtain $n \sim 6\times10^{13}$ cm^{-3}. The preexponential factor in Eq. (5c) therefore implies $\sigma_{n0}\eta \sim 4\times10^{-17}$ or $\eta \sim 0.04$, again a reasonable value.

We conclude therefore that the enhanced migration can be reasonably accounted for via an energy release mechanism. Let us therefore consider each of the two cases in more detail. Consider again first the hole-capture process, illustrated in Fig. 9(b). Electron capture (over the barrier $E_{\sigma n}$) causes the atom to distort to position Q'. Upon hole capture (over the barrier $E_{\sigma p}$) the atom has the additional vibrational energy E_R to assist it over the barrier E_B. E_R is therefore equal to $E_g - E_D + E_{\sigma p}$.

In the saturated injection region (hole-capture limited) $E_\sigma = E_{\sigma p}$ and the activation energy in Eq. (8a) reduces to $E_B - (E_g - E_D)$, assuming $E_B > E_R$. With $E_B = 1.2 \pm 0.1$ eV, the experimentally observed activation energy for recovery in the absence of injection,[40,41] and $E_g = 1.22$ eV,[42] the observed activation energy under saturation injection (0.27 eV) gives $E_D \sim 0.3$ eV. If $E_R > E_B$, the exponent in Eq. (8b) becomes $E_{\sigma p} = 0.27$ eV and $E_D < 0.3$ eV. This mechanism therefore predicts[47]

$$E_D \gtrsim 0.3 \text{ eV}.$$

For migration in the neutral charge state, Fig.

9(a), electron capture supplies $E'_R = E_D + E_{on}$ to assist the atom over the barrier E'_B in the neutral state. In the minority-carrier-limited regime, $E_\sigma = E_{on}$. For $E'_B > E'_R$, Eq. (8a) therefore predicts $E'_B - E_D = 0.14$ eV, the observed activation energy under these injection conditions, Eq. (5c). If $E'_B < E'_R$, $E_{on} = 0.14$ eV. In neither case can an estimate be made of E_D without knowledge of E'_B, if this is the operative mechanism.

From Eq. (11) we deduce that the onset of saturation recovery conditions at an injected current density $J \sim 1$ A/cm^2 is occurring at an electron density of $\sim 6\times10^{14}$ cm^{-3}. The electron density under laser injection may also be estimated. Assuming complete conversion to electron-hole pairs, the optical absorption coefficient of 13.7 cm^{-1} and laser intensity of ~ 50 W/cm^2 (3.75W, effective beam-spot area ~ 0.07 cm^2) give $\sim 6\times10^{21}$ (electron-hole pairs)/cm^3. Assuming a lifetime of $\sim 10^{-6}$ sec, this gives a minority carrier density of $\sim 6\times10^{15}$ cm^{-3}. Therefore, laser injection should be well into the saturation regime, consistent with the observations in Figs. 5 and 7. The reduced recovery rate in the more heavily irradiated sample of Fig. 7 could result from either majority-carrier removal or minority-carrier lifetime reduction.

We conclude that the enhanced recovery is consistent with an energy-release mechanism. The efficiency factor η is of the order of 0.1, implying a highly efficient conversion of energy to the diffusive mode. We cannot distinguish, however, whether the motion is occurring upon electron or hole capture. These mechanisms could be distinguished in counter-doped (n-type) material where the neutral donor state could be studied directly in DLTS. Also, of course, in such material, EPR might identify the configuration of the neutral state directly. Experiments of this type are being prepared.

4. Model

Our results appear consistent therefore only with an energy-release mechanism at the single donor level of the interstitial aluminum. Such a mechanism implies a configurational instability associated with a change of charge state at the neutral donor level. There is a logic to this: One of us (G.D.W.) has previously pointed out that there may be a tendency for "interstitialcy," bonded, configurations for an interstitial atom wherever the atom involved has partially filled p orbitals.[48] This reflects the inherent degeneracy of p orbitals in a position of high symmetry such as the "normal" tetrahedral (T_d) interstitial site. This, together with the strong coupling of p orbitals to distortions of the internuclear framework (i.e., their important role in molecular binding) may produce large static Jahn-Teller distortions, causing the atom to move out of its high-symmetry position.

As a free ion Al^{++} has a $3s^1$ configuration and, consistent with this, interstitial Al_i^{+} is observed by EPR to be in the T_d site. Al^{+} has a $3s^2$ configuration and Al^0, $3s^23p$. This simple rule therefore predicts that Al_i^+ will remain tetrahedral but Al_i^0 may tend to move out of this site into a lower-symmetry configuration. (Confirmatory evidence of this effect is available from EPR studies of interstitial carbon[30] and boron[12] in silicon also produced by irradiation. EPR has been observed for C_i^+ and B_i^0, both of atomic s^2p configuration, and low-symmetry configurations are found for both.) Direct confirmation of this for Al_i^0 would be highly desirable and the experiments mentioned above for counterdoped (n-type) material should answer this question.

5. Relevance to interstitial silicon

What we are learning about interstitial aluminum may also possibly serve as a guide to understanding the mysterious properties of interstitial silicon. As mentioned in the introduction, interstitial silicon, at least during electron irradiation in p-type material, appears to be extremely mobile, even at 4.2 K. Only interstitials trapped by impurities have been found so far by EPR. This suggests *athermal* ionization-enhanced motion, driven by recombination of the carriers generated during irradiation.

Silicon lies next to aluminum in the Periodic Table and as an interstitial therefore might also be expected to provide two donor levels. However, silicon has an additional electron and it would be the second donor state $Si_i^+(3s^23p)/Si_i^{++}(3s^2)$ which would provide the configurational instability. This perhaps explains the enhanced mobility in p-type material. Otherwise, the process would be the same but with the additional small but important difference that for interstitial silicon the delicate energy balance between E_R and E_B, already very close for interstitial aluminum, has switched to *athermal*, $E_R > E_B$.

Clues such as this are important simply because we are forced at present to have *only* clues. The high mobility of interstitial silicon means that it may not be possible to freeze it out and study it directly. Instead, we may be looking at the next best thing, a *trapped* interstitial, for that is how interstitial aluminum was formed.

C. Relation to previous work

Cherki and Kalma[49] have reported a deep level at $\sim E_V + 0.4$ eV from photoconductivity studies

which they suggested to be associated with interstitial aluminum. By studying dichroic behavior under uniaxial stress, they concluded that the defect had C_{3v} symmetry. Recognizing that EPR had already established T_d symmetry for Al_i^+, they suggested that the configuration might be that for Al_i^0, distorted for reasons similar to our arguments in Sec. IV B 4. Actually, we feel there are sufficient ambiguities in the interpretation of their results to make their identification uncertain. (Al_i^0 should not give rise to hole photoconductivity, boron-doped materials were observed to give a similar defect with the same thermal stability, now known to be inconsistent with EPR, etc.) We will therefore not attempt to correlate our results with theirs at this stage. It is interesting, however, that they were led to the conclusion of this instability.

Devine and Newman[50] reported the result, surprising at the time, that after the long 35 °C irradiations required for compensating heavily aluminum-doped silicon ($\sim 10^{19}$ cm^{-3}), no isolated Al_i^+ was observed, only $Al_i^+ Al_s^-$ pairs. They argued that this could probably be accounted for by normal thermally activated diffusion over the long times of the irradiations. Our present results for ionization-enhanced migration now provide a much simpler explanation of their observation.

V. CONCLUSION

We have observed for the first time recombination-enchanced migration of a defect normally stable at room temperature in silicon. This defect has been identified as interstitial aluminum, with its second donor state at $E_V + 0.17$ eV. We have presented evidence that this enhanced migration is due to recombination at the as yet unobserved single donor level of the interstitial aluminum. The mechanism is found to involve conversion of the energy released upon carrier capture into migrational energy of the interstitial aluminum atom. It is a very energy efficient process with at least 0.9 eV extracted from the carrier-capture energy to assist in the motion. It is also highly efficient in the conversion of this energy to the enhanced diffusion process.

We have suggested that the configurational instability associated with a change in charge state at the first donor level arises from the characteristic instability of the s^2p configuration for neutral aluminum which tends to make it Jahn-Teller distort out of the symmetric T_d interstitial site. Similar arguments for interstitial silicon suggest a corresponding instability at the second donor state which could explain its apparent long-range athermal migration during electron irradiation.

ACKNOWLEDGMENTS

We are indebted to Dr. A. O. Evwaraye for supplying many of the sample diodes used in the DLTS studies and for providing room-temperature electron irradiation of both diodes and EPR samples. Dr. Evwaraye's advice in the original assembly of the DLTS equipment is also gratefully acknowledged. Helpful discussions with Mr. R. D. Harris are gratefully acknowledged. One of us (J.R.T.) would like to thank the Sherman Fairchild Foundation for fellowship support. This research was supported by the U. S. Navy ONR Electronics and Solid State Science Program, Contract No. N00014-76-C-1097.

[1]L. C. Kimerling, Solid State Electron. 21, 1391 (1978).
[2]J. C. Bourgoin and J. W. Corbett, Radiat. Eff. 36, 157 (1978).
[3]A. M. Stoneham, Philos. Mag. 36, 983 (1977).
[4]P. J. Dean and W. J. Choyke, Adv. Phys. 26, 1 (1977).
[5]D. V. Lang and L. C. Kimerling, Phys. Rev. Lett. 33, 489 (1974).
[6]L. C. Kimerling and D. V. Lang, Inst. Phys. Conf. Ser. 23, 589 (1975).
[7]D. V. Lang, L. C. Kimerling, and S. Y. Leung, J. Appl. Phys. 47, 3587 (1976).
[8]D. V. Lang and L. C. Kimerling, Appl. Phys. Lett. 28, 248 (1976).
[9]D. V. Lang, Inst. Phys. Conf. Ser. 31, 70 (1977).
[10]W. T. Stacy and B. J. Fitzpatrick, J. Appl. Phys. 49, 4765 (1978).
[11]B. L. Gregory, J. Appl. Phys. 36, 3765 (1965).
[12]G. D. Watkins, Phys. Rev. B 12, 5824 (1975).
[13]G. D. Watkins, J. R. Troxell, and A. P. Chatterjee, Inst. Phys. Conf. Ser. 46 (to be published).
[14]G. D. Watkins, Chin. J. Phys. 15, 92 (1977).
[15]L. C. Kimerling, IEEE Trans. Nucl. Sci. NS-23, 1497 (1976).
[16]L. C. Kimerling, Inst. Phys. Conf. Ser. 31, 221 (1977).
[17]J. R. Troxell and G. D. Watkins, Bull. Am. Phys. Soc. 23, 214 (1978).
[18]A. P. Chatterjee, J. R. Troxell, and G. D. Watkins, Bull. Am. Phys. Soc. 23, 214 (1978).
[19]G. D. Watkins, in *Radiation Damage in Semiconductors* (Dunod, Paris, 1965), p. 97.
[20]J. C. Bourgoin and J. W. Corbett, Phys. Lett. 38A, 135 (1972).
[21]D. V. Lang, J. Appl. Phys. 45, 3014, 3023 (1974).
[22]G. L. Miller, D. V. Lang, and L. C. Kimerling, Annu. Rev. Mater. Sci. 7, 377 (1977).
[23]The dosimetry for these irradiations was only approximate. The absolute values of the fluences could be in error by a factor of 2 but their relative values are reliable.
[24]G. G. MacFarlane, T. P. McLean, J. E. Quarrington,

and V. Roberts, Phys. Rev. 111, 1245 (1958).
[25]A. M. Portis, Phys. Rev. 100, 1219 (1955); University of Pittsburgh, Sarah Mellon Scaife Radiation Laboratory Technical Note No. 1, 1955 (unpublished).
[26]M. Weger, Bell Syst. Tech. J. 39, 1013 (1960).
[27]*In situ* irradiations of ion implanted junction samples at liquid-helium temperatures currently in progress produce DLTS spectra which we have correlated with the isolated silicon vacancy and interstitial aluminum, as previously found in EPR studies. Upon thermal recovery of the vacancy around 170 K the $H2$ level is found to grow in with identical kinetics. Thus it appears that the $H2$ level may involve a vacancy complexed with some other defect.
[28]Estimates such as these which come from the temperature dependence of the various parameters in Eq. (2), reflect the extrapolated energy-level position to $T=0$.
[29]G. D. Watkins and J. W. Corbett, Phys. Rev. 138, A543 (1965).
[30]G. D. Watkins and K. L. Brower, Phys. Rev. Lett. 36, 1329 (1976).
[31]K. L. Brower, Phys. Rev. B 1, 1908 (1970).
[32]G. D. Watkins, Phys. Rev. 155, 802 (1967).
[33]The aluminum $G19$ pairs and the $G21$ defect are not normally in their EPR charge states in the p-type material. The spectra must be generated by light (through a germanium filter, $h\nu \lesssim 0.6$ eV for the $G21$ spectrum and through a water filter $h\nu > 1.0$ eV for the aluminum pairs). The fact that the sum of the three observed interstitial aluminum related spectra remains roughly constant through the anneal indicates that our photogeneration process is revealing essentially all of these defects.
[34]G. D. Watkins, Inst. Phys. Conf. Ser. 23, 1 (1975).
[35]L. C. Kimerling, H. M. DeAngelis, and J. W. Diebold, Solid State Commun. 16, 171 (1975).
[36]A. O. Evwaraye, J. Appl. Phys. 48, 734 (1977).
[37]F. Lüty, in *Physics of Color Centers*, edited by W. Beall Fowler (Academic, New York, 1968), p. 182.
[38]The equality of the capture and emission rates also means that the Fermi level is close to the defect level at $E_V + 0.17$ eV at room temperature.
[39]It will be demonstrated in Sec. IV B 3 (iii) that at the onset of saturation (~ 1 A/cm^2), the minority-carrier concentration is more than an order of magnitude smaller than the majority-carrier concentration. As a result, the identification of saturated injection with complete conversion to the neutral state is justified.
[40]The Fermi level at 100–200 °C, where recovery in the absence of injection was studied, is above the $E_V + 0.17$ eV level and the recovery therefore reflects the properties of the single positively charged state.
[41]An alternate mechanism for the recovery under short-circuit conditions is enhanced migration due to the presence of *thermally* generated minority carriers. If this process were the dominant one, the measured activation energy would be ~ 1.47 eV (the sum of the band gap, 0.14 eV for the minority-carrier-limited regime, Eq. (5c), and ~ 0.11 eV arising from the T^3 dependence of the combined density of conduction-band valence-band states) which is not observed. Estimates of the magnitude of this effect indicate, however, that it is only a factor of ~ 10 lower than the observed recovery rate at 200 °C the highest temperature studied, and it may therefore be contributing.
[42]The activation energies are estimated experimentally from the temperature dependence of the recovery rates and therefore reflect the extrapolated values at $T=0$. Therefore we use $E_g(T=0) = 1.22$ eV [H. G. Grimmeiss, Annu. Rev. Mater. Sci. 7, 341 (1977)].
[43]C. H. Henry and D. V. Lang, Phys. Rev. B 15, 989 (1977).
[44]J. D. Weeks, J. C. Tully, and L. C. Kimerling, Phys. Rev. B 12, 3286 (1975).
[45]Weeks *et al.* and Kimerling treated the case where the carrier capture rate was equal to the recombination rate R. Equation (7) is more general, including also the possibility that emission processes are operative where $C > R$.
[46]C. H. Henry, H. Kukimoto, G. L. Miller, and F. R. Merritt, Phys. Rev. B 7, 2499 (1973).
[47]In preliminary DLTS experiments with graded junctions, where majority carrier traps can be seen on the n-type side as well, a level at $E_C - 0.2$ eV has been detected in irradiated diodes. It also recovers under injection. This therefore might be the neutral donor state level.
[48]G. D. Watkins, Inst. Phys. Conf. Ser. 16, 228 (1973).
[49]M. Cherki and A. H. Kalma, Phys. Rev. B 1, 647 (1970).
[50]S. D. Devine and R. C. Newman, J. Phys. Chem. Solids 31, 685 (1970).